

Design of miniaturized patch crossover based on superformula slot shapes

Mutaz Akram Banat, Nihad Ibrahim Dib

Department of Electrical Engineering, Jordan University of Science and Technology, Irbid, Jordan

Article Info

Article history:

Received Oct 30, 2021

Revised Apr 8, 2022

Accepted May 5, 2022

Keywords:

Crossover
Microstrip patch
Superformula shapes

ABSTRACT

In this paper, miniaturized microstrip crossover circuits are proposed using slots shapes obtained using the superformula. The design starts by using a conventional half-wavelength square patch crossover. For miniaturization purposes, different superformula slot shapes are introduced on the square patch. The proposed crossovers are designed to operate at 2.4 GHz using a 0.8 mm thick FR-4 substrate with a relative permittivity of 4.4. The designs are simulated using the high frequency structure simulator (HFSS). One of the miniaturized designs is fabricated and its scattering parameters are measured using a vector network analyzer. Simulated and measured results agree very well. At the design frequency, the measured input port matching is better than -19 dB, while S_{12} , S_{13} and S_{14} have the values of -12 dB, -2.2 dB and -10 dB, respectively. Furthermore, a 71% size reduction is achieved as compared to the conventional crossover area.

This is an open access article under the [CC BY-SA](https://creativecommons.org/licenses/by-sa/4.0/) license.



Corresponding Author:

Mutaz Akram Banat

Department of Electrical Engineering, Jordan University of Science and Technology

P. O. Box 3030, Irbid 22110, Jordan

Email: mutazbanat@yahoo.com

1. INTRODUCTION

The performance of wireless communications systems is usually affected by the large fluctuations in the wireless signals which are caused by multi-path fading and interference. One way to overcome this is to use smart antenna arrays. The capacity and range of the base-station can be improved by the use of switched beam systems, which consist of fixed beamforming networks, without any modifications at the mobile unit. The key component of such beamforming networks is the Butler matrix which is widely used in smart antenna systems [1], [2]. Butler matrix is a passive reciprocal network that consists of couplers, phase-shifters, and crossovers. One of the common problems in microwave integrated circuits is the crossing transmission lines (TLs). To overcome this problem, crossover circuits are used whenever an intersection between TLs carrying different signals at the same layer is unavoidable. Traditionally, air-bridges and wired vias, which lead to non-planar structures and increase the fabrication complexity and cost, were used to design crossovers [3], [4]. To overcome this, planar four ports crossover circuits that allow a pair of intersecting lines to cross each other while achieving the required isolation between the two signal paths can be used.

Fully planar cascaded hybrids were proposed in [5], while, in [6], zero-dB directional couplers were designed. Symmetric four-port networks with good isolation between adjacent ports were presented in [7]–[9]. The main disadvantage of such crossovers is the large occupational area at low frequencies on printed circuit board (PCB) that limits their use in different applications. Therefore, several miniaturization techniques were introduced to overcome this while maintaining the same performance in [10]–[14]. The use of microstrip branch-line couplers (BLCs) for crossover applications was proposed in [10], where the goal

was to find the impedance values to get the crossover operation of the BLC. Using multi-section BLC enhances the performance and the bandwidth, but it suffers from several drawbacks, like its large size. New compact BLC shapes were investigated to overcome these disadvantages. In [11], the proposed crossover design used four arc-shaped slots and two perpendicular rectangular slots on the patch which resulted in 82% reduction in the total size compared with the conventional crossover. In [12], a dual-band branch-line coupler was presented where the BLC transmission lines were replaced by their equivalent T-/Pi-shaped networks. A similar approach was used in [13] to design a miniaturized crossover. Dual-band planar crossover with two-section BLC structure was proposed in [14], while, in [15], a multi-section BLC for crossover applications was presented. Based on negative-refractive-index transmission line metamaterial lines, a miniaturized crossover, with good performance, was proposed in [16]. In [17], a new planar dual-frequency crossover was presented. In [18], a wideband crossover was presented based on the typical 2x2 distributed window-shaped structure, while a miniaturized quad-band BLC crossover was proposed in [19]. In [20], a transmission line model was proposed and used in the design of compact single and two-section BLCs at 0.85 GHz. In [21], wideband crossovers with high selectivity were proposed based on stub-loaded ring resonators.

In this paper, the design of miniaturized patch crossover based on superformula slot shapes is investigated. Different superformula slot shapes are proposed. The overall crossover occupation area reduced by a factor of 71% of its original size.

2. RESEARCH METHOD

The conventional square crossover is shown in Figure 1. To design any crossover, the insertion loss (between the opposite ports) should be minimized and the isolation (between adjacent ports) should be maximized while maintaining compactness. In Figure 1, the microstrip patch along with the ground plane on the other side of the substrate can be represented as a dielectric loaded cavity with perfect electric top and bottom walls [22]. The thickness of the substrate is assumed to be very small compared to the wavelength and the patch dimensions, thus, the only possible field configuration inside the cavity is the transverse magnetic (TM) mode. The electric and magnetic fields inside the cavity can be written in terms of the TM_{mn0} modes as (1), (2), (3) [23]:

$$E_z = A_1 \cos(m\pi x/L) \cos(n\pi y/L) \quad (1)$$

$$H_x = A_2 \cos(m\pi x/L) \sin(n\pi y/L) \quad (2)$$

$$H_y = A_3 \sin(m\pi x/L) \cos(n\pi y/L) \quad (3)$$

where A_i are the amplitudes of the field's components, L is the length of the patch, and m , and n are the mode numbers. Thus, the resonant frequency of the two fundamental modes TM_{100} and TM_{010} is given as (4):

$$f_r = \frac{c}{2L\sqrt{\epsilon_r}} \quad (4)$$

where ϵ_r is the substrate relative permittivity and c is the free-space speed of light. The magnetic field components for the TM_{100} mode are:

$$H_y = A_3 \sin(\pi x/L), H_x = 0. \quad (5)$$

for the TM_{010} mode, they are:

$$H_x = A_2 \sin(\pi y/L), H_y = 0. \quad (6)$$

It is clear that these two modes have orthogonal magnetic fields. Based on the Poynting vector [24], the signal flows in y -direction for the TM_{010} mode and in x -direction for the TM_{100} mode. Each face-to-face pair of crossover ports (ports 1 and 3, or ports 2 and 4) must be properly aligned to couple one of the above modes, which will maximize the isolation between the adjacent ports and will minimize the insertion loss between the opposite ports.

2.1. Conventional square patch crossover design and experimental results

Assuming a resonant frequency of 2.4 GHz, the initial dimensions of the conventional square patch crossover shown in Figure 1 are calculated using (4). Using FR-4 substrate (thickness 0.8 mm and $\epsilon_r=4.4$)

and 50Ω characteristic impedance for all ports, the following optimized dimensions are obtained: $W=64.7 \text{ mm}$, $L=30.7 \text{ mm}$, $W_f=1.53 \text{ mm}$. The total area for this crossover excluding the feeding lines is 9.4 cm^2 . A picture of the fabricated crossover is shown in Figure 2. The design is simulated using the high frequency structure simulator (HFSS), the simulated results are shown in Figure 3 and the measured ones which were obtained using an E5071C ENA Keysight vector network analyzer are shown in Figure 4. At the design frequency, simulated S-parameters: S_{11} , S_{12} , S_{13} and S_{14} have the values of -28 dB, -15 dB, -1.4 dB and -15 dB, respectively. The measured results show S_{11} better than -28 dB at the design frequency. The experimental transmission parameters, S_{12} , S_{13} , and S_{14} are -14.5 dB, -2 dB and -16.5 dB at 2.4 GHz, respectively. Table 1 shows the values of the simulated and measured S-parameters at 2.4 GHz.

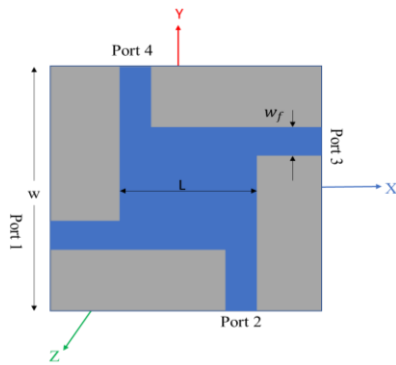


Figure 1. Conventional square microstrip patch crossover

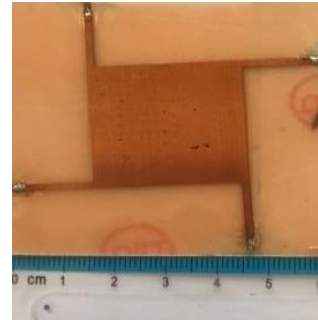


Figure 2. Picture of the fabricated conventional crossover

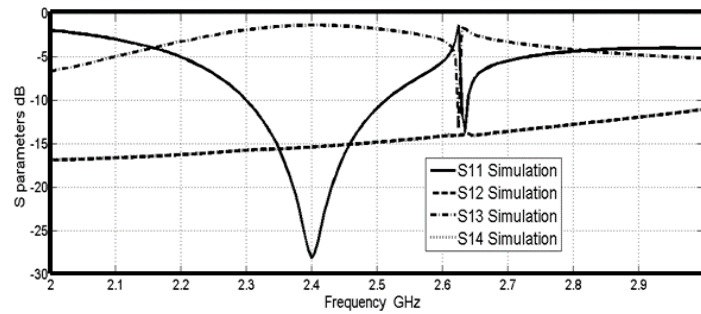


Figure 3. Simulated S-parameters of the crossover shown in Figure 2

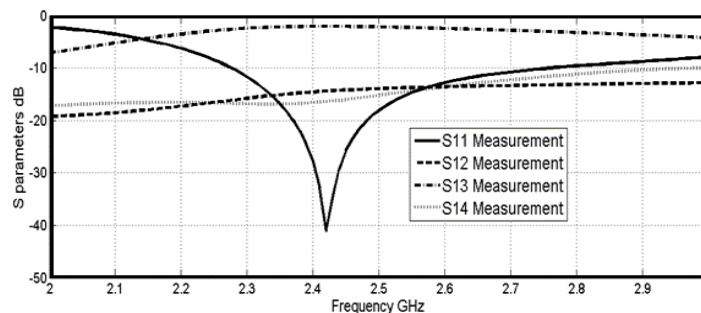


Figure 4. Measured S-parameters of the crossover shown in Figure 2

Table 1. Measured and simulated S-parameters comparison at 2.4 GHz

	S_{11} (dB)	S_{12} (dB)	S_{13} (dB)	S_{14} (dB)
Simulated	-28	-15	-1.4	-15
Experimental	-28	-14.5	-2	-16.5

2.2. Miniaturized square crossover using superformula shapes

In order to reduce the overall conventional crossover area, multiple slots shapes were investigated like perpendicular lines and circular slot shape as proposed in [11]. In this paper, we use the superformula generated slot shape. To the authors knowledge, the superformula was not used before to miniaturize the crossover circuit. The superformula, known also as Gielis formula, is a geometrical expression that allows to generate many geometrical shapes and forms [25]. The superformula expression contains seven different parameters: a , b , $N_{1,2,3}$ and $m_{1,2}$ and it is given by the polar function of the form $f=r(\phi)$:

$$r(\phi) = \left[\left| \frac{1}{a} \cos\left(\frac{m_1}{4}\phi\right) \right|^{N_2} + \left| \frac{1}{b} \sin\left(\frac{m_2}{4}\phi\right) \right|^{N_3} \right]^{-1/N_1} \quad (7)$$

The parameters a and b are chosen with different values to vary the distance of the inflection points from the origin. The parameters N_2 and N_3 control the concavity of the curves between points, corners, and sectors. The parameters $m_{1,2}$ determine the number of points, corners, and sectors. Figure 5 shows different shapes using different parameters values.

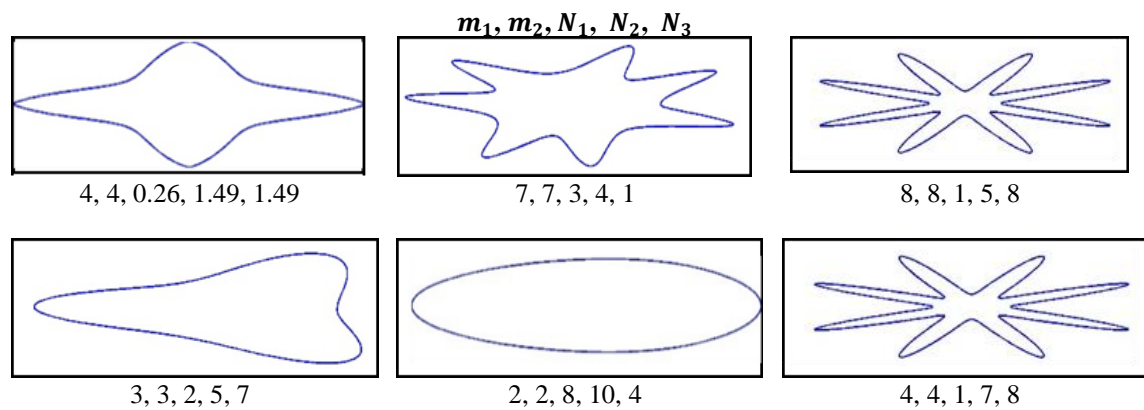


Figure 5. Examples of superformula shapes ($a=1, b=1$)

3. RESULTS AND DISCUSSION

3.1. Design #1

The first superformula slot shape is generated by using (7) with the following parameters, $a=b=1, m_1=m_2=3, N_1=5, N_2=N_3=18$. Figure 6 shows the HFSS layout for the proposed compact crossover design with dimensions: $W=53$ mm, $L=19$ mm and $W_f=1.53$ mm. As shown in Figure 7, at the design frequency, the simulated S-parameters: S_{11}, S_{12}, S_{13} and S_{14} have the values of -47 dB, -10 dB, -2.3 dB and -8 dB, respectively. The total area for this crossover excluding the ports dimensions is 3.6 cm^2 , which is equivalent to 38% of the conventional crossover size. In the next sections, different superformula shapes will be investigated.

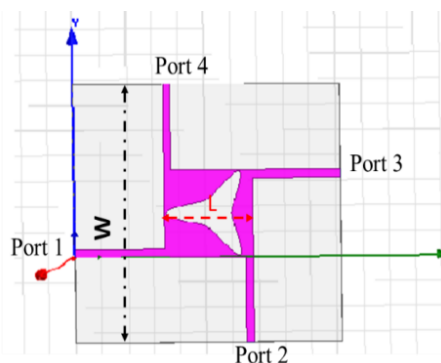


Figure 6. HFSS layout of a miniaturized crossover using superformula slot shape (design #1)

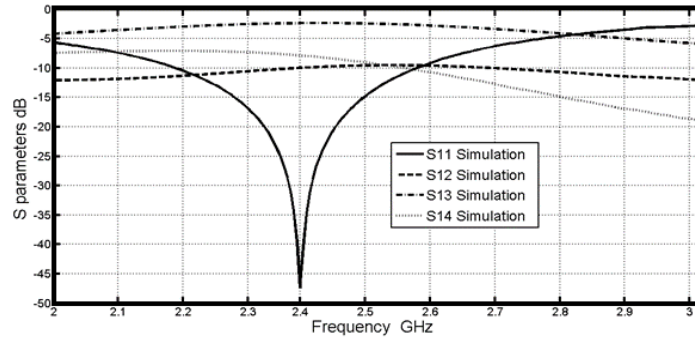


Figure 7. Simulated S-parameters of the miniaturized crossover shown in Figure 6

3.2. Design #2

The second superformula slot shape is generated by using (7) with the following parameters, $a = b = 0.8$, $m_1=m_2 = 8$, $N_1 =3$, $N_2 = 4$, $N_3 = 7$. Figure 8 shows the HFSS layout for the proposed miniaturized crossover circuit with dimensions: $W=52$ mm, $L=18$ mm and $W_f=1.53$ mm. The simulated scattering parameters are shown in Figure 9. At the design frequency, S_{11} , S_{12} , S_{13} and S_{14} have the values of -21.5 dB, -10 dB, -1.9 dB and -9.5 dB, respectively. The total area for this crossover excluding the ports dimensions is 3.2 cm^2 which is equivalent to 34% of the conventional crossover size.

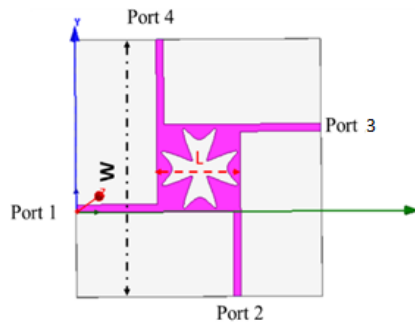


Figure 8. HFSS layout of a miniaturized crossover using superformula slot shape (design #2)

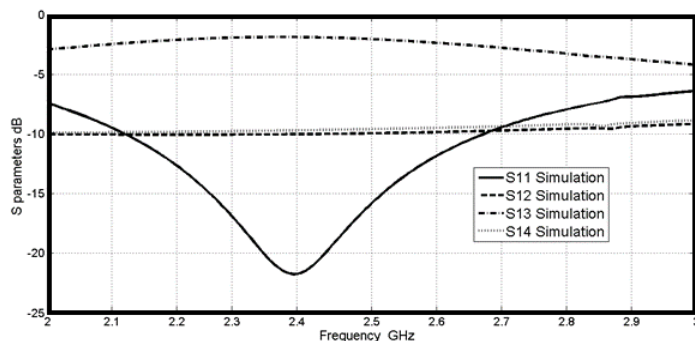


Figure 9. Simulated S-parameters of the miniaturized crossover shown in Figure 8

3.3. Design #3

In this section, another superformula slot shape is investigated in order to achieve better performance results and more size reduction. The slot shape is a combined one between the superformula shape ($a = b = 1$, $m_1=m_2 = 4$, $N_1 = 0.26$, $N_2 = N_3 = 1.49$) and two perpendicular rectangular slots with some scaling to get the required resonant frequency. Figure 10 shows the HFSS layout for the proposed miniaturized crossover with dimensions: $W=50.5$ mm, $L=16.5$ mm and $w_2=0.2$ mm. Figure 11 shows the

simulated scattering parameters. At the design frequency, S_{11} , S_{12} , S_{13} , and S_{14} have the values of -21 dB, -11 dB, -1.8 dB and -10.6 dB, respectively. The total area for this crossover excluding the ports dimensions is 2.7 cm^2 which is equivalent to 29% of the conventional crossover size.

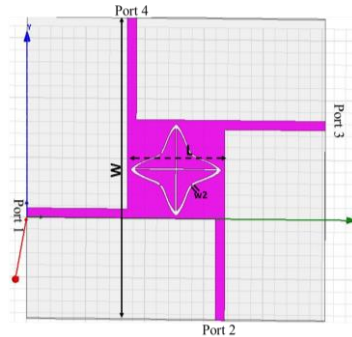


Figure 10. HFSS layout of a miniaturized crossover using superformula slot shape (design #3)

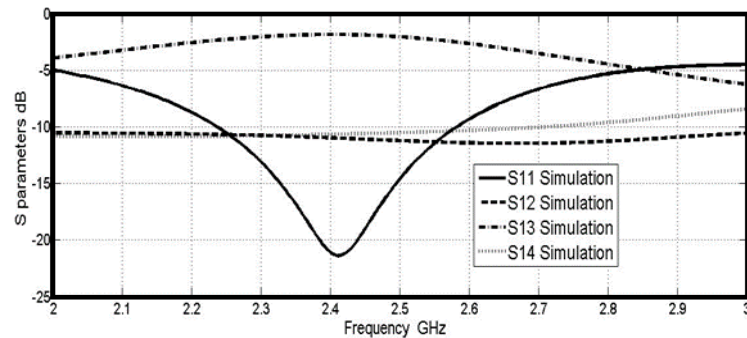


Figure 11. Simulated S-parameters of the miniaturized crossover shown in Figure 10

This last crossover design is fabricated in Figure 12. Figure 13 presents the measured scattering parameters, which shows a S_{11} better than -26 dB at the design frequency. The experimental transmission parameters, S_{12} , S_{13} , and S_{14} are -12 dB, -2.2 dB and -10.5 dB at 2.4 GHz, respectively. Table 2 shows a comparison between the above three superformula slot shapes performance and the size reduction compared with the conventional square crossover using the same substrate and the resonant frequency. Table 3 shows a comparison between the proposed miniaturized crossover (design #3) and some recently published crossovers. For fair comparison, the area for each design is given in terms of the guided wavelength at the design frequency.

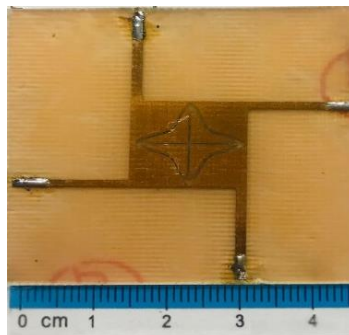


Figure 12. Picture of the fabricated miniaturized crossover using superformula slot shape (design #3)

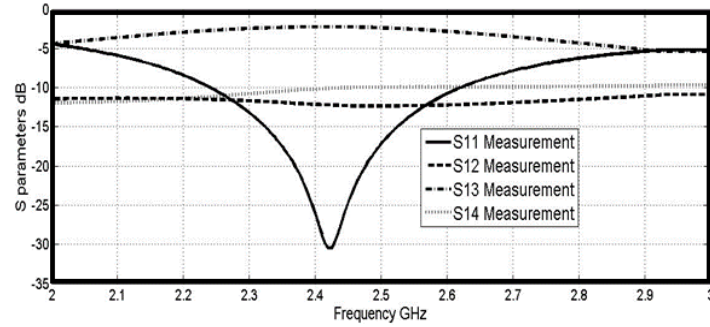


Figure 13. Measured S-parameters of the miniaturized crossover shown in Figure 12

Table 2. A comparison between the simulated results of different miniaturization techniques of conventional crossover

Miniaturization Method	S_{11} (dB)	S_{12} (dB)	S_{13} (dB)	S_{14} (dB)	Size (cm^2)	Size reduction compared with the conventional
Design #1	-47	-10	-2.3	-8	3.6	62%
Design #2	-21.5	-10	-1.9	-9.5	3.2	66%
Design #3	-21	-11	-1.8	-10.6	2.7	71%
Conventional square crossover	-26	-17	-1.4	-17	9.4	NA

Table 3. Comparison of proposed crossover (design #3) with other published designs.

Ref	Substrate	Frequency (GHz)	S_{11} (dB)	S_{12} (dB)	S_{13} (dB)	Size($\lambda_q \times \lambda_q$)
[23]	Rogers (thickness 0.64 mm & $\epsilon_r=10.2$)	5.5	-25	-13	-0.9	(0.5x0.5)
[26]	Rogers (thickness 0.64 mm & $\epsilon_r=10.2$)	2.4	-27	-17	-1	(0.45x0.45)
[27]	Rogers (thickness 0.508 mm & $\epsilon_r=3.55$)	2.4	-17	-22	-1	(0.3x0.3)
[28]	Rogers (thickness 0.508 mm & $\epsilon_r=2.65$)	1.78	-22	-28	-0.6	(0.4x0.28)
[29]	Rogers (thickness 0.635 mm & $\epsilon_r=10.2$)	2.1-2.75	-11	-19	-1	(0.6x0.6)
Design #3	FR-4 Epoxy (thickness 0.8 mm & $\epsilon_r=4.4$)	2.4	-21	-11	-1.8	(0.27x0.27)

4. CONCLUSION

In this paper, the physical area of the conventional microstrip patch crossover was reduced by 71% using slot shapes inspired and further optimized through the utilization of superformula based geometries. A very good agreement between the simulated and measured results was obtained. In general, the proposed miniaturized crossovers have very good performance at the design frequency, and thus, can be used in beamforming networks.

ACKNOWLEDGEMENTS

The authors are grateful to Eng. Nadia Tanash and Eng. Jehan Sheyyab from JUST EE Department for their assistance during the fabrication and measurement stages. Special thanks for Eng. Omar Jibreel for his advice and support throughout this work.

REFERENCES




- [1] E. T. Der, T. R. Jones, and M. Daneshmand, "Miniaturized 4×4 butler matrix and tunable phase shifter using ridged half-mode substrate integrated waveguide," *IEEE Transactions on Microwave Theory and Techniques*, vol. 68, no. 8, pp. 3379–3388, Aug. 2020, doi: 10.1109/TMTT.2020.2989798.
- [2] J. M. Wen, C. K. Wang, W. Hong, Y. M. Pan, and S. Y. Zheng, "A wideband switched-beam antenna array fed by compact single-layer butler matrix," *IEEE Transactions on Antennas and Propagation*, vol. 69, no. 8, pp. 5130–5135, Aug. 2021, doi: 10.1109/TAP.2021.3060040.
- [3] G. E. Ponchak and E. Tentzeris, "Development of finite ground coplanar (FGC) waveguide 90 degree crossover junctions with low coupling," in *2000 IEEE MTT-S International Microwave Symposium Digest (Cat. No.00CH37017)*, 2000, vol. 3, pp. 1891–1894, doi: 10.1109/MWSYM.2000.862351.
- [4] W. Liu, Z. Zhang, Z. Feng, and M. F. Iskander, "A compact wideband microstrip crossover," *IEEE Microwave and Wireless Components Letters*, vol. 22, no. 5, pp. 254–256, May 2012, doi: 10.1109/LMWC.2012.2190270.
- [5] J. S. Wight, W. J. Chudobiak, and V. Makios, "A microstrip and stripline crossover structure (letters)," *IEEE Transactions on Microwave Theory and Techniques*, vol. 24, no. 5, pp. 270, May 1976, doi: 10.1109/TMTT.1976.1128838.
- [6] D. V. Kholodniak and I. B. Vendik, "A novel type of 0-dB directional coupler for microwave integrated circuits," in *29th European Microwave Conference, 1999*, Oct. 1999, pp. 341–344, doi: 10.1109/EUMA.1999.338370.
- [7] Y. Chen and S.-P. Yeo, "A symmetrical four-port microstrip coupler for crossover application," *IEEE Transactions on Microwave*

Design of miniaturized patch crossover based on superformula slot shapes (Mutaz Akram Banat)




- Theory and Techniques*, vol. 55, no. 11, pp. 2434–2438, Nov. 2007, doi: 10.1109/TMTT.2007.908675.
- [8] F.-L. Wong and K.-K. M. Cheng, “A novel, planar, and compact crossover design for dual-band applications,” *IEEE Transactions on Microwave Theory and Techniques*, vol. 59, no. 3, pp. 568–573, Mar. 2011, doi: 10.1109/TMTT.2010.2098883.
- [9] A. Abbosh, S. Ibrahim, and M. Karim, “Ultra-wideband crossover using microstrip-to-coplanar waveguide transitions,” *IEEE Microwave and Wireless Components Letters*, vol. 22, no. 10, pp. 500–502, Oct. 2012, doi: 10.1109/LMWC.2012.2218586.
- [10] J. Yao, C. Lee, and S. P. Yeo, “Microstrip branch-line couplers for crossover application,” *IEEE Transactions on Microwave Theory and Techniques*, vol. 59, no. 1, pp. 87–92, Jan. 2011, doi: 10.1109/TMTT.2010.2090695.
- [11] B. Henin and A. M. Abbosh, “Compact planar microstrip crossover for beamforming networks,” *Progress In Electromagnetics Research C*, vol. 33, pp. 123–132, 2012, doi: 10.2528/PIERC12081515.
- [12] M. A. Maktoomi, M. S. Hashmi, and F. M. Ghannouchi, “Systematic design technique for dual-band branch-line coupler using T- and Pi-networks and their application in novel wideband-ratio crossover,” *IEEE Transactions on Components, Packaging and Manufacturing Technology*, vol. 6, no. 5, pp. 784–795, May 2016, doi: 10.1109/TCPMT.2016.2548498.
- [13] H. A. Mohamed and A. S. Mohra, “Compact cascaded branch line coupler using T-sections conversion,” in *2017 34th National Radio Science Conference (NRSC)*, Mar. 2017, pp. 64–70, doi: 10.1109/NRSC.2017.7893478.
- [14] F. Lin, Q.-X. Chu, and S. W. Wong, “Dual-band planar crossover with two-section branch-line structure,” *IEEE Transactions on Microwave Theory and Techniques*, vol. 61, no. 6, pp. 2309–2316, Jun. 2013, doi: 10.1109/TMTT.2013.2261084.
- [15] S. P. Yeo and N. Deng, “Multi-section branch-line couplers for crossover application,” *Microwave and Optical Technology Letters*, vol. 59, no. 7, pp. 1625–1629, Jul. 2017, doi: 10.1002/mop.30595.
- [16] M. A. B. Abbasi, M. A. Antoniadis, and S. Nikolaou, “A compact microstrip crossover using NRI-TL metamaterial lines,” *Microwave and Optical Technology Letters*, vol. 60, no. 11, pp. 2839–2843, Nov. 2018, doi: 10.1002/mop.31458.
- [17] S. Menon, “Microstrip patch antenna assisted compact dual band planar crossover,” *Electronics*, vol. 6, no. 4, Sep. 2017, doi: 10.3390/electronics6040074.
- [18] S. Zhang and S. Sun, “Modified window shape-based crossover with enhanced bandwidth,” *International Journal of RF and Microwave Computer-Aided Engineering*, vol. 31, no. 2, Feb. 2021, doi: 10.1002/mmce.22503.
- [19] R. K. Barik, Q. S. Cheng, N. C. Pradhan, and K. S. Subramanian, “A miniaturized quad-band branch-line crossover for GSM/WiFi/5G/WLAN applications,” *AEU - International Journal of Electronics and Communications*, vol. 134, May 2021, doi: 10.1016/j.aeu.2021.153611.
- [20] J.-W. Wu, J.-Y. Ke, C. F. Jou, and C.-J. Wang, “Microstrip-fed broadband circularly polarised monopole antenna,” *IET Microwaves, Antennas & Propagation*, vol. 4, no. 4, 518, Apr. 2010, doi: 10.1049/iet-map.2008.0400.
- [21] C. Zhao, W. Feng, and W. Che, “High selectivity wideband filtering crossovers using stub-loaded ring resonators,” *Journal of Electromagnetic Waves and Applications*, vol. 30, no. 7, pp. 860–870, May 2016, doi: 10.1080/09205071.2016.1159997.
- [22] C. A. Balanis, *Antenna theory: analysis and design*, John Wiley & sons, 2015.
- [23] A. M. Abbosh, “Planar wideband crossover with distortionless response using dual-mode microstrip patch,” *Microwave and Optical Technology Letters*, vol. 54, no. 9, pp. 2077–2079, Sep. 2012, doi: 10.1002/mop.27028.
- [24] D. K. Cheng, *Field and wave electromagnetics*, Pearson Education India, 1989.
- [25] J. Gielisi, “A generic geometric transformation that unifies a wide range of natural and abstract shapes,” *American Journal of Botany*, vol. 90, no. 3, pp. 333–338, Mar. 2003, doi: 10.3732/ajb.90.3.333.
- [26] B. Henin and A. Abbosh, “Design of compact planar crossover using Sierpinski carpet microstrip patch,” *IET Microwaves, Antennas & Propagation*, vol. 7, no. 1, pp. 54–60, Jan. 2013, doi: 10.1049/iet-map.2012.0262.
- [27] Y.-Y. Lin, B.-L. Jiang, C.-Y. Huang, and C.-W. Tang, “Design of a wideband planar patched crossover with slotted lines,” in *2017 IEEE Asia Pacific Microwave Conference (APMC)*, Nov. 2017, pp. 280–282, doi: 10.1109/APMC.2017.8251433.
- [28] W. Feng, T. Zhang, and W. Che, “Compact single-band planar crossover based on coupled lines,” in *2016 46th European Microwave Conference (EuMC)*, Oct. 2016, pp. 975–978, doi: 10.1109/EuMC.2016.7824508.
- [29] B. Henin and A. Abbosh, “Wideband planar microstrip crossover with high power handling capability and low distortion,” *Microwave and Optical Technology Letters*, vol. 55, no. 2, pp. 439–443, Feb. 2013, doi: 10.1002/mop.27335.

BIOGRAPHIES OF AUTHORS



Mutaz Akram Banat    received the B. Sc. degree in electrical engineering from Jordan University of Science and Technology, Irbid, Jordan, in 2012. He received the MSc degree in electrical engineering with the major of Wireless Communication from Jordan University of science and Technology, Irbid, Jordan, in 2022. His research interests include the computational electromagnetics, antennas, analysis and design of passive microwave components, and optimization techniques. He can be contacted at email: mutazbanat@yahoo.com.



Nihad Ibrahim Dib    obtained his B. Sc. and M.Sc. in electrical engineering from Kuwait University in 1985 and 1987, respectively. He obtained his Ph.D. in EE (major in Electromagnetics) in 1992 from University of Michigan, Ann Arbor. Then, he worked as an assistant research scientist in the radiation laboratory at the same school. In Sep. 1995, he joined the EE department at Jordan University of Science and Technology (JUST) as an assistant professor and became a full professor in Aug. 2006. His research interests are in computational electromagnetics, antennas, and modeling of planar microwave circuits. He can be contacted at email: nihad@just.edu.jo.